# The Feel of MEMS Barometers: Inexpensive and Easily Customized Tactile Array Sensors

# Share Your Story

# Inexpensive and Easily Customized Tactile Array Sensors using MEMS Barometers Chips

Yaroslav Tenzer, Leif P. Jentoft, Robert D. Howe

Harvard School of Engineering and Applied Sciences

*Abstract*—This paper presents a new approach to the construction of tactile array sensors based on barometric pressure sensor chips and standard printed circuit boards. The chips include tightly integrated instrumentation amplifiers, analog-to-digital converters, pressure and temperature sensors, and control circuitry that provides excellent signal quality over standard digital bus interfaces. The resulting array electronics can be easily encapsulated with soft polymers to provide robust and compliant grasping surfaces for specific hand designs. The use of standard commercial-off-the-shelf technologies means that only basic electrical and mechanical skills are required to build effective tactile sensors for new applications. Performance evaluation of prototype arrays demonstrate excellent linearity (<1% typical) and low noise (<0.01 N). External addressing circuitry allows multiple sensors to communicate on the same bus at over 100 Hz per sensor element. Sensors can be mounted as close as 3x5 mm spacing, and spatial impulse response tests show that solid-mechanics based signal processing is feasible. This approach promises to make sensitive, robust, and inexpensive tactile sensing available for a wide range of robotics and human-interface applications.

## I. Introduction

Tactile sensing is widely considered an essential capability for effective grasping and manipulation [1], [2], [3]. Parameters such as the location of object contacts on the robot hand and contact pressure distribution are believed to be essential for effective manipulation in unstructured environments. Yet despite decades of research and the availability of several commercial tactile array sensors, there has been little experimental progress in using tactile information to control grasping and manipulation.

There are many reasons for the lack of headway in this area, but a major factor is certainly the cost and complexity of integrating tactile sensing into robot hands. Hundreds of touch sensing devices have been published in the robotics literature, but building such sensors requires custom fabrication using nonstandard techniques [1], [2], [3].

Commercial tactile array sensors avoid the need to master exotic fabrication technologies, but they are typically costly, fragile, and cover only a limited area of a hand [4], [5], [6]. Both custom-built and commercial sensors require considerable engineering effort to integrate into the contact surfaces of a new robot hand, and there are further challenges in developing the multiplexing, cabling, and digitizing to get the sensor signals down the robot arm and into the control computer.

This paper presents a new method for tactile array construction and integration. The approach takes advantage of
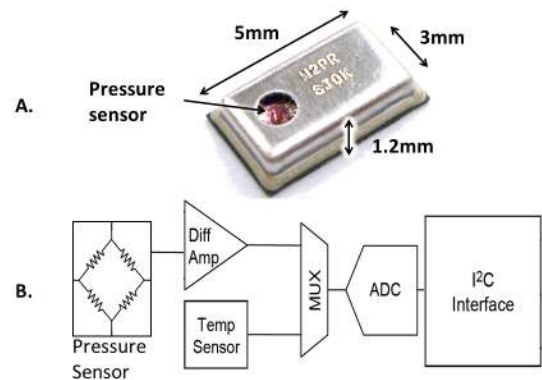


Figure 1. MPL115A2 sensor from Freescale Semiconductor, and the block diagram of the device.

recently-available miniature barometric sensor chips, which include a MEMS pressure sensor, temperature sensor, instrumentation amplifier, analog-to-digital converter, and standard bus interface, all for as little as US$1 per sensor. These devices can be mounted on standard printed circuit boards (rigid or flexible) using standard IC surface-mount techniques. The circuit boards can be mounted to robot fingers and easily over-molded with rubber to provide robust grasping surfaces. The resulting tactile array sensors have moderate spatial resolution (3-5 mm), and excellent sensitivity (<0.01 N), linearity (<1%), and bandwidth (>100 Hz). In the following section we describe the sensor chips and their integration into tactile arrays. In particular, we present solutions to two key issues: extending address limitations to enable connection of multiple sensors onto one bus at high bandwidth, and adapting the rubber molding process to provide high contact sensitivity. We then present experimental characterization of a prototype array sensor in terms of force magnitude, spatial, and temporal response. We conclude with a discussion of design considerations and the implications for robot manipulation research.

## II. Tactile Array Integration

### A. Barometric Sensors

Barometric sensor chips were developed for consumer products such as desktop weather stations and GPS systems, where altimeters can improve vertical positioning accuracy [7]. As such, these sensors have a small footprint, low power consumption, and are mass produced at low cost. Several versions are available, all sharing the combination of a MEMS
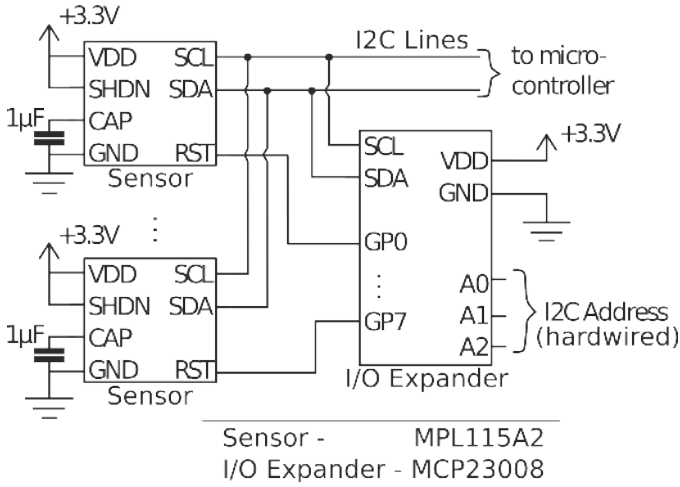
Figure 2. An example of the use of auxiliary circuits to enable connection of up to eight barometric sensors on the same I2C bus.
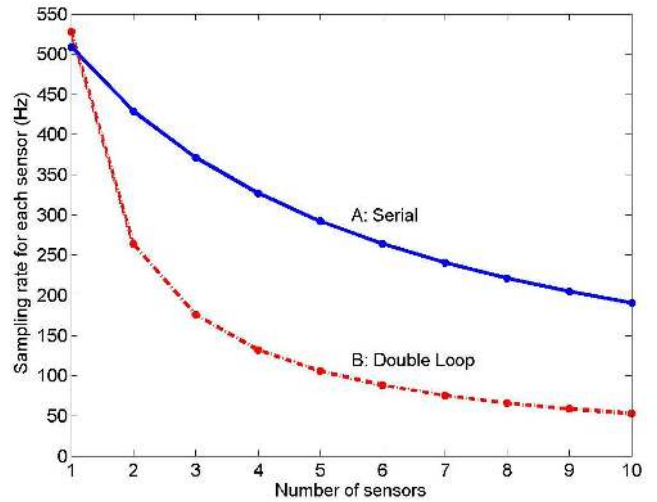


Figure 3. Theoretical sampling rates of an array with I2C bus speed of 400kHz. A) Serial approach where for each sensor the system commands to start conversion, waits till the data is available (1.6 ms), and then reads the data. B) Double loop (i.e. alternating start conversion and read sensor) approach utilizing the waiting time to communicate the start-conversion command to other sensors in the array.

transducer with integrated signal conditioning and bus interface in a standard surface mount IC package (e.g. [8], [9]). In this paper we focus on the MPL115A2 sensor (Freescale Semiconductor Inc., Austin, TX, USA). This device (Fig. 1) has a miniature 5x3x1.2 mm package, uses the I2C bus protocol [10] and, at the time of writing, is the least expensive alternative. These sensors have an air pressure range of 50-115 kPa with a resolution of 0.15 kPa. This sensor also has a relatively large ventilation hole (1 mm diameter) directly above the pressure sensor. This is advantageous for rubber casting, as described below.

### B. Circuitry Design and Rubber Casting

A number of steps are required to adapt the barometric sensors for tactile applications. First, circuitry and programming protocols are required to access multiple sensors over the I2C bus because all sensors are manufactured with the same preassigned I2C address. Chip select can be implemented through the RST pin, which disables the I2C interface when driven low [9]. This is preferable to applying and removing power, as required for some alternative chips, because it avoids the power-up delay that would greatly limit sampling rates. In the circuit example in Fig. 2, the RST pin of up to eight sensors are controlled by an I/O expander (MCP23008, Microchip Technology Inc., Chandler, AZ, USA). Multiple I/O expanders can share the I2C bus with the sensors, so a total of only two communication wires and two power lines are required to communicate to an array of hundreds of sensors. Arrays with large number of sensors would require the use of I/O expanders with larger addressing range and extra I/O pins (e.g. PCA9671, NXP Semiconductors, Eindhoven, The Netherlands).

The sensor array sampling speed was calculated based on the performance characteristics of the sensors, the I/O expander, and the bus communication speed; here we use the chip maximum of 400 kHz. The main performance bottleneck is the sensor data conversion time of 1.6 ms, which is the minimum interval between the start convert command and data available in the internal registers. Two different algorithms

were developed to scan an array of sensors. The first is a serial approach, where the controller sends the start-convert command to a sensor, waits for the conversion time interval, and then reads the data. The time to scan an array is

$$\left(\frac{C_{bits} + S_{bits} + R_{bits}}{bus\,speed} + T_c\right) \cdot N$$

where $C_{bits}$ is the number of bits required to command the IO expander to select a single barometer chip, $S_{bits}$ is the number of bits required to command data conversion, $R_{bits}$ is the number of bits required to read the data, $T_c$ is the conversion time of the sensors, and $N$ is the number of sensors in the array. The second algorithm utilizes the waiting time to communicate the start-conversion command to other sensors in the array, then returns to each sensor after the appropriate interval and reads the data. Using this double loop method the array sampling time is

$$\left(\frac{2C_{bits} + S_{bits} + R_{bits}}{bus\,speed}\right) \cdot N + T_c$$

The performance of the algorithms is shown in Fig. 3. The second algorithm is about three times as fast for the selected eight sensor example in Fig. 2 with a 400 kHz bus speed, and about four times as fast for a 22 sensor array, which is currently under development for a robotic finger.

The second issue requiring special attention is casting of the sensors in rubber. Rubber forms a robust and compliant contact surface for grasping and manipulation, and serves to communicate surface contact pressure within the layer of rubber to the ventilation hole and thus to the MEMS transducer. Encapsulation of the array can be readily accomplished by suspending the circuit board with mounted sensors in a mold and pouring in liquid polymer. When molding is performed at atmospheric pressure, however, air is trapped within the sensor chip behind the ventilation hole. This results in low sensitivity
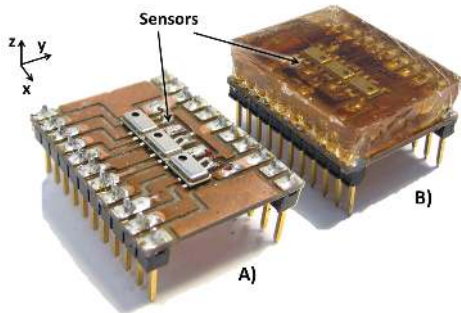
Figure 4. Sensors layout in the experimental setup. A: Before cast. B: In 6mm rubber.

because surface pressure produces only small changes in the volume of the trapped air below the ventilation hole.

One solution is to remove the top of the sensor metal case, so the rubber directly encapsulates the MEMS pressure transducer. This improves sensitivity but requires nonstandard chip handling techniques. We also found that this exposes fragile components such as bond wires that can break when large forces are applied to the rubber surface.

A more successful approach is vacuum degassing. The mold is placed in a vacuum chamber (e.g. standard laboratory bell jar) immediately after the rubber is poured, and the air is removed with a vacuum pump. This removes the air from inside the sensors, thus allowing the rubber to enter the case though the ventilation hole. Post casting dissection of a number of sensors showed that the rubber fills the sensor without damaging internal structures.

In the supplementary multimedia materials for this paper, we include an example implementation of a tactile array sensor created using this approach [11]. This sensor array has 8 columns and 5 rows with 6 mm spacing. On-board microcontrollers handle sensor addressing and I2C-to-USB conversion. The material includes schematics, PCB layout, and microprocessor firmware.

## III. Sensor Characterization Methods

To experimentally characterize the performance of the proposed tactile array, three sensors were soldered in a line at 5 mm spacing to a rigid printed circuit board (PCB) (Fig. 4); this is the closest obtainable spacing for sensors mounted end-to-end in the longest dimension. Three PCBs were then cast in rubber with thicknesses of 4, 6, and 10 mm, which spans the typical range of rubber covering for robot fingers. The rubber was a two-part room temperature curing polyurethane elastomer (VytaFlex 20, Smooth-On, Inc., Easton, USA). This inexpensive rubber has low viscosity for mixing and pouring, is compliant but mechanically robust after curing, and is compatible with shape deposition manufacturing (SDM) prototyping techniques which have proved useful for robot hand construction [12]. Its modulus of elasticity was experimentally confirmed to be 280 kPa.

Communication with the sensors was through a USB-to-I2C bridge interface (CY3240, Cypress Semiconductor Corporation, San Jose, CA, USA). The pressure values from the sensors were calibrated using algorithms provided by the sensor

manufacturer, including gain and temperature correction [9]. The compensation algorithm was modified so that the final result was not rounded or scaled for atmospheric pressure.

Sensitivity of the resulting sensor arrays was evaluated by applying a load to the rubber directly above the ventilation hole using a probe with spherical tip with diameter of 6 mm. The probe was attached to a triple beam balance with about 0.001 N resolution. The load was applied incrementally until the sensor output saturated. Then, the load was gradually removed to evaluate the hysteresis of the sensor. The typical interval between load changes was 30 sec, and total interval for loading and unloading of each sensor was approximately ten minutes. The process was repeated for each sensor in each array for the three rubber thickness.

The step response was evaluated by pre-loading the sensors to 50% of the saturation load through a probe with spherical tip with diameter of 6 mm, and then quickly removing the load in under 10 ms. Pressure readings were sampled at 125 Hz.

Noise and temperature drift were evaluated by recording outputs of both pressure and temperature at 30 Hz for 1000 sec, at ambient temperatures between 20 and 26 degrees Celsius, which bounds the duration of most simple grasping and manipulation tasks at around room temperature. All three sensors in each of the three arrays were sampled with no applied load. The spatial response of the sensors was measured in terms of the impulse response. A constant force was applied sequentially along the line of sensors while the output was recorded for each sensor. To avoid the need for precise alignment, we used a line load oriented perpendicular to the line of sensors, i.e. a narrow metal probe with negligible width in the $x$ direction (along the line of sensors, as shown in Fig. 4) but wider than the rubber pad in the perpendicular $y$ direction.

## IV. Results and Discussion

The sensitivity measurements show excellent linearity and no visible hysteresis (Fig. 5). For each rubber thickness, the three lines represent readings from the three sensors in the array. The plot shows one symbol for loading and one for unloading at every value for the applied load for each of the nine sensors; these symbols are typically so close that they are visually indistinguishable. The results show a highly linear behavior for most of the measurement range, where the coefficient of determination $r^2 > 0.99$ for all sensors and the maximum deviation from linearity was 2.2% for 4 mm, 1.3% for 6 mm, and 0.4% for 10 mm rubber. The average variability in sensitivity for test arrays was 4.4% and the maximum observed was 11.5% for 4 mm rubber. One cause of the observed variation may be due to limited manual alignment accuracy between the sensor port and probe.

The useful pressure measurement range appears to be larger than stated in the datasheet: the mean of the outputs at the saturation is 775.3 counts, corresponding to a calibrated air pressure of 149.2 kPa, well above the datasheet maximum of 115 kPa. The effects of regularly exceeding the specified maximum is not clear; our prototypes have shown no degradation in performance under thousands of loading cycles, and under repeated loads above ten times saturation.
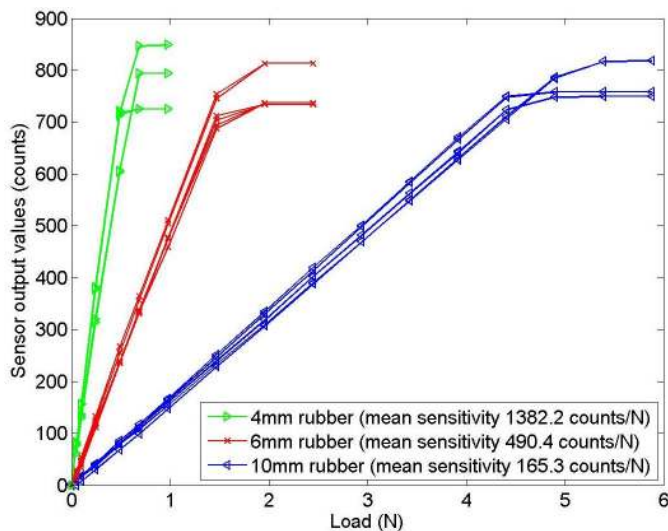
Figure 5. Sensor output values versus applied surface load for rubbers of different thickness. The three lines per rubber thickness represent offset corrected readings from the three sensors in each array. Symbols indicate the output from each sensor during loading and unloading cycles.



Figure 7. Variation in pressure output (shown as the mean of the values) as a function of temperature for different rubber thicknesses, and values from a calibrated sensor without rubber for reference. Lines are best fits ($r^2 > 0.99$)
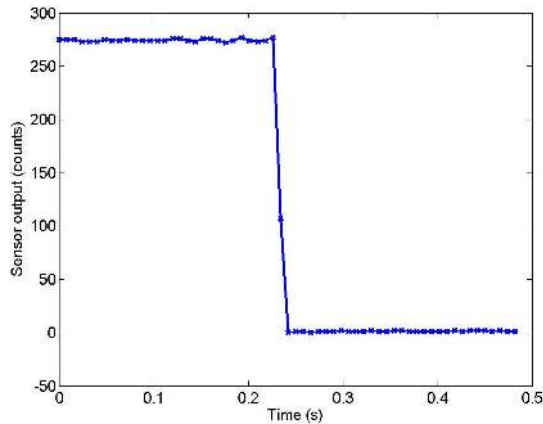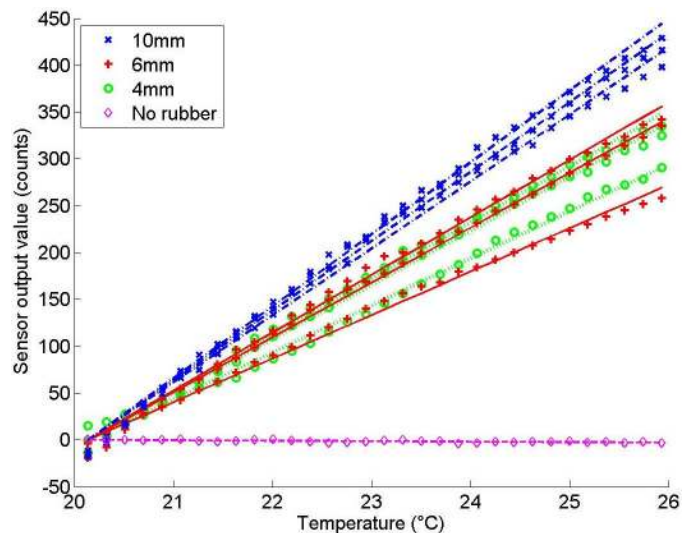


Figure 6. Step change in load for a sensor in 10 mm rubber. The line represents offset corrected reading during unloading of the sensor.

Sensor output in step tests showed fast response and no hysteresis; an example from a sensor under 10 mm rubber is shown in Fig. 6. The full step response invariably occurs within two samples or 16 ms. The negligible hysteresis level is expected for a system with force (or pressure) input and output. If the input was specified as a position step, hysteresis would likely have been evident in the sensor output, but the behavior under force loads seems most germane to robotic manipulation applications, where forces must be controlled for grasping and manipulation. In any case, the hysteretic properties depend on the properties of the elastomer used for encapsulation, and could be limited if needed through careful choice of materials.

Sensor output variation with ambient temperature is highly linear ($r^2 > 0.99$ for all sensors) over the range of 20-26 degrees Celsius (Fig.7). The manufacture provides a temperature compensation algorithm using the on-board temperature sensor (see [9]), but it is not accurate for sensors cast in rubber, probably due to the differences in thermal expansion coef-

ficients. The observed linearity suggests that a simple linear compensation scheme is adequate, although high accuracy may require determination of the specific calibration coefficient for each sensor.

The signal noise was recorded from all nine unloaded sensors in the three arrays at 100 Hz for 60 seconds. The overall average root-mean-square noise was 1.27 counts with standard deviation of 0.1 counts. This corresponds to an applied load of 0.0077 N, 0.0026 N, and 0.00092 N for rubbers of 10, 6 and 4 mm respectively, where the sensitivity was calculated using the measured ratios from Fig.5. These noise levels are small with respect to the measurement range of the sensor, and simple filtering can further reduce the effects of the noise; for example, we were able reliably detect a one gram load on the 6 mm array with a 10 Hz bandwidth.

Power spectrum analysis suggests that the noise is homogeneously distributed across frequencies. We observed variations in noise level as a function of the capacitor value (Fig.2), with higher capacitance reducing noise, which may have an impact on the response time. The results reported here used the recommended capacitor value of $1 \mu F$) [9].

The spatial impulse response from an array of sensors for different rubber thickness is presented in Fig.8. The results show that as rubber thickness grows, the strain distribution grows but the sensor loses sensitivity. Some variation in output values and curve amplitude between the sensor readings can be observed, and these also may be attributed to the alignment accuracy of the setup.

Fig.9 shows the impulse response from a single sensor in 6 mm of rubber, and the theoretically predicted curve for the subsurface vertical normal stain distribution at the sensor depth (from [13]). The rubber thickness for the theoretical curve was adjusted with respect to the thickness of the sensor (i.e. 1.2 mm), and the amplitude of the curve has been fitted to the experimental data.

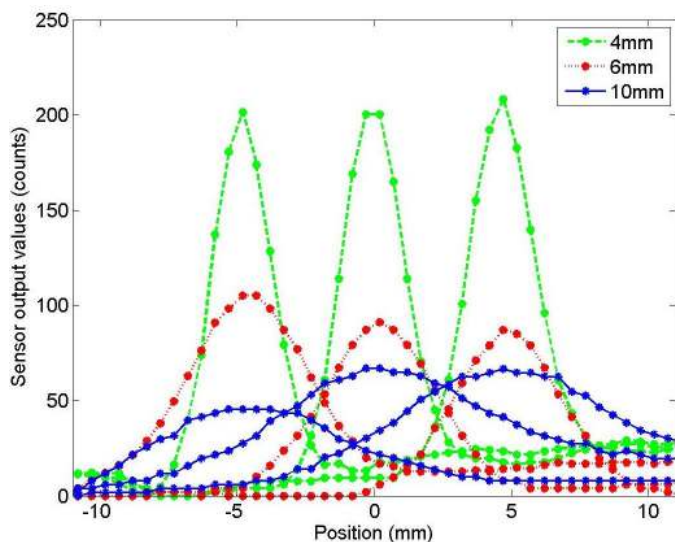The calculated and experimental curves show close agree-

Figure 8. Spatial response to a scanned normal impulse for three sensors in each array with with different rubber thicknesses.
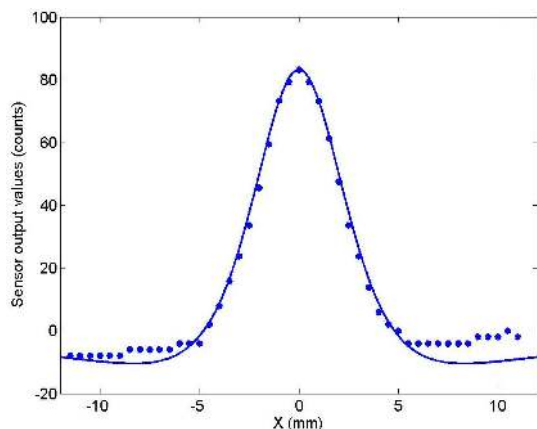


Figure 9. Single sensor response for an impulse normal to the surface for 6mm rubber, and the theoretically predicted curve [13]. Sensor values were offset corrected, and the theoretical curve magnitude (but not spatial dimension) was scaled to the data.

ment, indicating that methods from solid mechanics (e.g. [13]) may be useful for analysis and interpretation of the sensor signals. The discrepancy between theoretical prediction (based on an infinite half-space model) and the data at the edges of the plot may be due to the irregular structures within the rubber, i.e. the rigid sensor package mounted on the PCB and the location of the MEMS sensor beneath the ventilation hole.

## V. CONCLUSIONS

This paper presents a new approach to the construction of tactile arrays based on barometric pressure sensor chips and standard printed circuit boards. The chips include tightly integrated instrumentation amplifiers, analog-to-digital converters, temperature sensors, and control circuitry that provides excellent signal quality over standard digital bus interfaces. The resulting electronic array can be easily encapsulated in soft polymers to adept the sensors to specific robot hand designs.

Performance evaluation of prototype arrays demonstrated excellent linearity (<1% typical) and low noise levels (<0.01 N). External addressing circuitry allows multiple sensors to communicate on the same bus at over 100 Hz per sensor element. Sensors can be mounted as close as 3x5 mm spacing, and spatial impulse response tests show that solid-mechanics based signal processing approaches are feasible [13]. The sensors also have temperature sensing capabilities, which can be useful for development of thermal sensing systems [14].

The use of standard commercial-off-the-shelf technologies means that only basic electrical and mechanical skills are required to build effective tactile sensors, and costs are low despite the high performance of the resulting sensor system. The sensor arrays circuits can be embedded in rubber using custom 3D-printed molds to integrate the sensors into robot finger structures with a robust and compliant grasping surface. This approach can enable new progress in understanding the role of tactile information in robotic grasping and manipulation, as well as research in diverse fields such as biomechanics and human-machine interfaces where contact location and pressure distribution information can be valuable.

## REFERENCES

[1] R. S. Dahiya, G. Metta, M. Valle, and G. Sandini, "Tactile Sensing - From Humans to Humanoids," *IEEE Transactions on Robotics*, vol. 26, no. 1, pp. 1–20, 2010.

[2] M. R. Cutkosky, R. D. Howe, and W. R. Provancher, "Force and Tactile Sensing," in *Springer Handbook of Robotics*, B. Siciliano and O. Khatib, Eds. Springer Berlin / Heidelberg, 2008, ch. 19.1, p. 1611.

[3] M. H. Lee and H. R. Nicholls, "Tactile sensing for mechatronics-a state of the art survey," *Mechatronics*, vol. 9, no. 1, pp. 1–31, 1999.

[4] "Pressure Profile Systems, Inc." [Online]. Available: http://www.pressureprofile.com/

[5] "Syntouch - The BioTac." [Online]. Available: http://www.syntouchllc.com/

[6] "Tactile Pressure Measurement, Tekscan Inc." [Online]. Available: http://www.tekscan.com/

[7] G. Lammel and J. Patzel, "Pressure Sensors provide indoor competency for navigation," *Small Times*, pp. 1–4, 2009.

[8] Bosh Sensortec, "BMP085 Digital Pressure Sensor," *Datasheet*, no. Oct, 2009.

[9] Semiconductor Freescale, "MPL115A2 Miniature I2C Digital Barometer," *Datasheet*, 2010.

[10] NXP Semiconductors, "UM10204 I2C-bus specification and user manual," *User Manual*, vol. 4, no. February, 2012.

[11] "Takktile Project. Open source tactile array." [Online]. Available: http://www.takktile.com

[12] A. M. Dollar and R. D. Howe, "A robust compliant grasper via shape deposition manufacturing," *IEEEASME Transactions on Mechatronics*, vol. 11, no. 2, pp. 154–161, 2006.

[13] R. S. Fearing and J. M. Hollerbach, "Basic solid mechanics for tactile sensing," *The International Journal of Robotics Research*, vol. 4, no. 3, pp. 266–275, 1984.

[14] H. R. Nicholls and M. H. Lee, "A Survey of Robot Tactile Sensing Technology," *The International Journal of Robotics Research*, vol. 8, no. 3, pp. 3–30, Jun. 1989. [Online]. Available: http://ijr.sagepub.com/content/8/3/3.abstract